

Potential inhibition of HIV-1 encapsidation by oligoribonucleotide–dendrimer nanoparticle complexes

Raveen Parboosing^{1,2}

Louis Chonco^{1,2}

Francisco Javier de la Mata^{3,4}

Thavendran Govender⁵

Glenn EM Maguire⁵

Hendrik G Kruger⁵

¹Department of Virology, University of KwaZulu-Natal, ²National Health Laboratory Service, Durban, South Africa;

³Organic and Inorganic Chemistry Department, University of Alcalá, Alcalá de Henares,

⁴Networking Research Center on Bioengineering, Biomaterials and Nanomedicine (CIBER-BBN), Madrid, Spain; ⁵Catalysis and Peptide Research Unit, University of KwaZulu-Natal, Durban, South Africa

Background: Encapsidation, the process during which the genomic RNA of HIV is packaged into viral particles, is an attractive target for antiviral therapy. This study explores a novel nanotechnology-based strategy to inhibit HIV encapsidation by an RNA decoy mechanism. The design of the 16-mer oligoribonucleotide (RNA) decoy is based on the sequence of stem loop 3 (SL3) of the HIV packaging signal (Ψ). Recognition of the packaging signal is essential to the encapsidation process. It is theorized that the decoy RNA, by mimicking the packaging signal, will disrupt HIV packaging if efficiently delivered into lymphocytes by complexation with a carbosilane dendrimer. The aim of the study is to measure the uptake, toxicity, and antiviral activity of the dendrimer–RNA nanocomplex.

Materials and methods: A dendriplex was formed between cationic carbosilane dendrimers and the RNA decoy. Uptake of the fluorescein-labeled RNA into MT4 lymphocytes was determined by flow cytometry and confocal microscopy. The cytoprotective effect (50% effective concentration [EC_{50}]) and the effect on HIV replication were determined in vitro by the methylthiazolyl diphenyl-tetrazolium bromide (MTT) assay and viral load measurements, respectively.

Results: Flow cytometry and confocal imaging demonstrated efficient transfection of lymphocytes. The dendriplex containing the Ψ decoy showed some activity (EC_{50} = 3.20 μ M, selectivity index = 8.4). However, there was no significant suppression of HIV viral load.

Conclusion: Oligoribonucleotide decoys containing SL3 of the packaging sequence are efficiently delivered into lymphocytes by carbosilane dendrimers where they exhibit a modest cytoprotective effect against HIV infection.

Keywords: packaging signal, dendrimers, transfection, antiretroviral, HIV packaging

Introduction

Encapsidation, the process by which the dimeric RNA of HIV is preferentially packaged by the Gag polypeptide into nascent virions, is an essential step in HIV-1 replication.^{1–4} This process involves interaction between the gag nucleocapsid protein p7 (NCp7) and a region of the HIV genome known as the packaging signal (Ψ). This interaction is an attractive target for antiviral therapy because the secondary structures of Ψ and nucleocapsid are highly conserved among retroviruses^{5–9} and mutations in NCp7 result in totally defective virions.^{10–12} This suggests that drug resistance to “packaging inhibitors” is less likely to develop. Furthermore, RNA export (ie, packaging) is a virus-specific and not a cellular process so that drugs targeting this step are likely to have a high therapeutic index.¹

Studies exploring the potential of targeting the packaging process have shown promising results. For example, vectors that express Ψ -containing transcripts,

Correspondence: Raveen Parboosing
Department of Virology, University of KwaZulu-Natal, 5th Floor Laboratory Building, Inkosi Albert Luthuli Central Hospital, 800 Bellair (Vusi Mzimele) Road, Mayville, Durban 4091, South Africa
Tel +27 31 240 2816
Fax +27 31 240 2797
Email parboosingr@ukzn.ac.za

or constructs that contain the packaging signal, interfere with packaging and successfully inhibit HIV replication in vitro.^{13–16} In another study, RNA ligands (“aptamers”) with Ψ -like sequences bound to NCp7 with high affinity and abrogated packaging (where the ligand, rather than the genome, is packaged, resulting in defective virions).¹⁷ Antisense RNA that targets the packaging signal inhibits retroviral replication.^{18,19}

Four “stem-loops”, SL1–4, constitute the secondary structure of Ψ ; of these, SL3 has been identified by mutational,^{10–12} biochemical,²⁰ SL-NCp7 affinity,^{21,22} ligand substitution²³ and nuclear magnetic resonance (NMR)²⁴ experiments to play a particularly important role in viral RNA packaging.²⁵ The aim of this study is to design and optimize a potential oligoribonucleotide antiviral therapeutic that will inhibit packaging by several possible mechanisms such as, 1) competitive inhibition: the oligoribonucleotide will compete with SL3 (and other SLs) for binding sites on NCp7; 2) decoy encapsidation: packaging of the oligoribonucleotide decoy, rather than the HIV genome, will reduce the pool of available NCp7 for Ψ binding and packaging;²⁶ 3) defective interfering particles,²⁷ and 4) interference with the role of NCp7 (especially as a “nucleic acid chaperone”) in other steps of replication, such as initiation of reverse transcription, strand transfer, integration, gag multimerization, RNA dimerization and viral assembly.^{1,4,6,7,28–30}

Lymphocytes, in particular, and suspension cell lines, in general, are, however, notoriously difficult to transfect.^{31,32} Nonetheless, there have been reports of successful transfection of lymphocytes using carbosilane dendrimers.^{33,34} This prompted us to investigate the potential of a carbosilane dendrimer to deliver the SL3 oligoribonucleotide decoy into CD4⁺ lymphocytes, thereby inhibiting the replication of HIV.

Materials and methods

Reagents

The following reagents were obtained through the NIH AIDS Reagent Program,^{35,36} Division of AIDS, NIAID, NIH: MT4 from Dr Douglas Richman and HIV_{IMB}/H9 from Dr Robert Gallo. The RNase-free, high-performance liquid chromatography (HPLC)-purified RNA construct was synthesized by Dharmacon (Pittsburgh, PA, USA). BLOCK-iT™ Fluorescent Oligo (used as control RNA) was obtained from Thermo Fisher Scientific (Waltham, MA, USA). Nuclease-free water was obtained from Qiagen (Hilden, Germany). Heat-inactivated fetal bovine serum (FBS) was obtained from BioChrom/Merck Millipore (Berlin, Germany). Optimem™ and GIBCO® Roswell Park Memorial Institute (RPMI) 1640 media (with or without phenol red) were obtained from Life Technologies (Carlsbad, CA, USA). Phosphate-buffered saline (PBS) without

Ca/Mg was obtained from Lonza (Basel, Switzerland). All other reagents were obtained from Sigma unless otherwise indicated.

Design of the RNA decoy

An oligoribonucleotide decoy containing a 16-mer sequence of SL3 (ACUAGCGGAGGCUAGA) was synthesized for use in this study (Figure 1). For uptake studies, the RNA was modified to include a fluorescein label at the 3' end. The design of the RNA decoy was based on, 1) the structure of Ψ , and its molecular interaction with NCp7, including NMR spectroscopy elucidation of its three-dimensional conformation,²⁴ 2) evidence from insertional mutagenesis,^{10–12,37–44} ligand binding^{17,23,45,46} and biochemical experiments^{20,21,41,47–50} regarding the factors (eg, the nucleotide sequence and content) that determine the affinity between Ψ and NCp7, 3) previous in vitro gene therapy experiments (using either aptamers¹⁷ or vectors^{14,16,18,19}) in which Ψ -like nucleotide sequences have successfully abrogated packaging, and 4) previous studies using archetypal SL3 ligands.⁴⁶ Systematic Evolution of Ligands by Exponential Enrichment (SELEX) ligands²³ and synthetic RNA stem loops.²¹

RNA preparation and handling

The custom-made RNA (16-mer sequence of SL3) was deprotected as recommended by the manufacturer,⁵¹ dried using a centrifugal evaporator (miVac DNA Sample Concentrator; Genevac, Stone Ridge, NY, USA), stored at -80°C as a pellet and resuspended in RNase-free deionized water just prior to use. RNase-free consumables were used, and precautions were taken to keep surfaces free from RNase (RNaseZap® wipes from Thermo Fisher Scientific). The RNA was quantified by measuring absorbance at 260 nm (adjusted for the effect of fluorescein) (BioSpec Nano; Shimadzu Corporation, Kyoto, Japan).

Dendrimer synthesis

A third-generation cationic carbosilane dendrimer was used for this study. This dendrimer contains 24 positive charges on

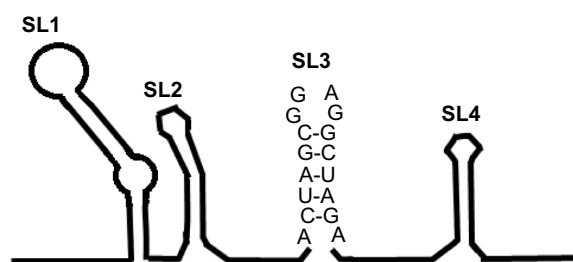


Figure 1 The four SLs that form the HIV-1 packaging signal.

Note: The 16-mer sequence of SL3 (ACUAGCGGAGGCUAGA), used in this study, is shown.

Abbreviation: SLs, stem loops.

its skeleton and terminal –OH groups that could participate in hydrogen bonds with biomolecules (Figure 2). The synthesis of this dendrimer has been previously reported and involves the initial synthesis of a carbosilane dendrimer decorated with terminal dimethyl amino groups and posterior quarternization with 2-iodoethanol.⁵²

Dendriplex formation and optimization

Dendriplexes were formed by mixing equal volumes of dendrimer and RNA (dissolved in RNase-free, deionized water), at varying molar ratios, and incubating for 15 minutes at room temperature, away from light. Freshly prepared dendriplexes (<1 hour old) were used to treat the cells. The ratio of dendrimer:RNA (\pm charge ratio) and the dose of the dendriplex were optimized in a series of experiments, based on the degree of complexation (gel retardation assay), uptake (flow cytometry and confocal microscopy), cytotoxic vs cytoprotective effect (methylthiazolyldiphenyl-tetrazolium bromide [MTT] assay) and effect on viral replication (viral load). The dendriplexes used in the uptake (flow cytometry and confocal microscopy) experiments were prepared by mixing 10 μ M RNA with the following serially diluted concentrations of dendrimer (bearing in mind that the dendrimer has 24 positive charges and the RNA 16 negative charges per

molecule, ie, P/N=3:2): dendriplex (8:1): 54 μ M; dendriplex (4:1): 27 μ M; dendriplex (2:1): 13.5 μ M and dendriplex (1:1): 6.75 μ M. In the MTT assay, serial dilutions of the dendrimer or dendriplex were used, beginning with the highest concentration of 75 μ M. In experiments where the control RNA was used, the concentration of dendrimer and \pm charge ratio was equivalent to that of the Ψ RNA.

Gel retardation assay

Complexation was studied in 2% agarose gel electrophoresis, using fluorescently labeled RNA and loading buffer.³³

Cells and virus

MT4 lymphocytes were grown in RPMI 1640 medium supplemented with 10% heat-inactivated FBS at 37°C in 5% CO₂. Cells were used at the exponential phase of growth and with viability at least 95%. The Countess™ automated Cell Counter (Thermo Fisher Scientific, Waltham, MA, USA) was used to determine cell counts and viability.

Stock virus was prepared by harvesting supernatant of HIV-infected MT4 lymphocytes at day 5 post-infection. The virus was titrated by conventional methods and stored at –80°C until use.⁵³ All work involving HIV culture was performed in the appropriate biosafety conditions.^{54,55}

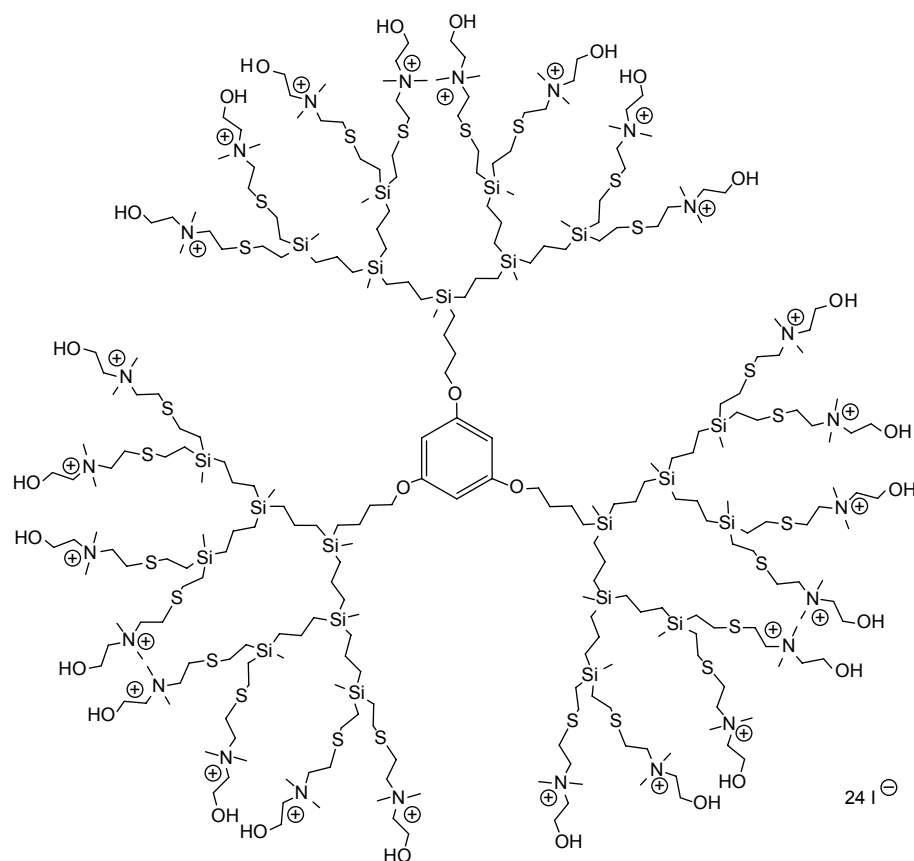


Figure 2 Third-generation cationic carbosilane dendrimer used in this study.

Flow cytometry

MT4 lymphocytes (150,000 cells/well) were suspended in wells of a microtiter plate with 200 μ L Optimem™. The cells were then incubated for 4 hours with 25 μ L of untreated control (Optimem™ only), RNA control (RNA only), dendrimer only (54 μ M), 10% dimethyl sulfoxide (DMSO; dead cell control) and dendriplexes at various molar ratios.⁵⁶ The cells were harvested, washed first with PBS, then with acid–glycine buffer for 30 seconds and finally again with PBS. The acid–glycine buffer (for the removal of dendriplexes bound to the surface of the cell membranes) consisted of 0.2 M glycine in PBS (adjusted to pH 3.0 by addition of hydrochloric acid).⁵⁷ The cells were then fixed with paraformaldehyde (at 4°C for 15 minutes) and then finally washed and resuspended in PBS. The cells were pelleted by gentle centrifugation after each wash step. The cells were stored at 4°C until analysis by flow cytometry (within 24 hours). The experiment was repeated without the acid–glycine wash to estimate the proportion of surface-bound vs intracellular RNA.

Uptake and viability were determined on BD FACS-Canto™ II (BD Biosciences, San Jose, CA, USA) instrument. To determine viability, 2 μ L of Zombie Aqua™ dye (Biolegend, San Diego, CA, USA) was added to cell suspensions prior to fixation, as per manufacturer's instructions. Uptake of RNA was quantified as the percentage of cells that took up fluorescein.

Confocal microscopy

Cells were treated, harvested and washed as for flow cytometry and then added to poly-L-lysine-coated microscope slides. The slides were fixed with paraformaldehyde and incubated for 10 minutes with Fluoroshield™ with 4',6-diamidino-2-phenylindole (DAPI) stain and then viewed and photographed under confocal microscope, ZEISS Confocal LSM 710 (Zeiss, Oberkochen, Germany).³⁴

MTT assay

The MTT assay to determine cytotoxicity (50% inhibitory concentration [IC₅₀]), cytoprotective (antiviral) effect (50% effective concentration [EC₅₀]) and selectivity index (SI) was performed in triplicate as previously described.⁵³ Briefly, MT4 lymphocytes were seeded in wells of a microtiter plate at 6×10^5 cells/mL and treated with serial dilutions of azidothymidine (AZT), dendrimer alone, dendriplex with control RNA or dendriplex with Ψ RNA. A total of 50 μ L of RPMI 1640 medium was added to each well in one half of the plate (mock infection), while 50 μ L of HIV_{IIIb} at 300 tissue culture infective dose (TCID₅₀) was added to the other half (HIV infection). The plate was incubated for 5 days at

37°C in 5% CO₂. At the end of the incubation period, the MTT assay was performed to assess toxicity in mock (uninfected) cells and cytoprotective effect in HIV-infected cells. The optical density readings were plotted on a graph, and the IC₅₀ and EC₅₀ were determined by linear extrapolation. Untreated, uninfected cells and untreated, HIV-infected cells were deemed to have 100% and 0% viability, respectively. Typically, the viability of the untreated, uninfected cells, as measured by the optical density reading, was at least fivefold that of untreated, HIV-infected cells.⁵³ Growth medium without phenol red was used in the assay to improve sensitivity of absorbance readings.

Viral load assay

MT4 cells were incubated for 3 hours with HIV_{IIIb}, at multiplicity of infection (MOI) 0.01, washed thrice with PBS to remove the initial inoculum and then plated at 3×10^5 cells/mL (200 μ L per well with RPMI 1640 medium and 10% FBS). Wells were treated in triplicate with 25 μ L of AZT, dendrimer alone, dendriplex with control RNA or dendriplex with Ψ RNA.⁵⁸ The concentration of the dendrimer was kept constant. A total of 25 μ L of RPMI 1640 medium was added to untreated control wells. After 3 or 5 days of incubation, 100 μ L was aspirated from each well, inactivated by exposure to acidified Triton X (in isopropanol) for 1 hour,⁵³ washed twice (by centrifugation and resuspension in PBS) and finally resuspended in 3 mL PBS for viral load quantification. The dilution factor (10^4) introduced because of the aforementioned procedures was taken into account when calculating the final viral load. Viral load was quantified by the automated Roche Cobas® 6800/8800 System (Roche Diagnostics, Mannheim, Germany) as per the manufacturer's instructions. This is a fully automated polymerase chain reaction (PCR)-based system with a linear range of 20–10,000,000 copies/mL.

Statistical analysis

Unpaired Student's *t*-test was used to calculate *P*-values. A *P*-value of <0.05 was regarded as significant.

Results

The oligoribonucleotide molecule formed complexes with the carbosilane dendrimer

Successful complexation was demonstrated on gel electrophoresis when the molar ratio of dendrimer:RNA exceeded 2 (corresponding to a \pm charge ratio of >3:1) (Figure 1). Faint bands appear at lower ratios, suggesting partial complexation (Figure 3).

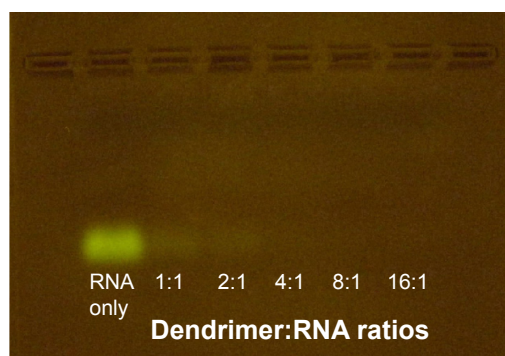


Figure 3 A 2% agarose electrophoresis gel showing RNA and carboxylated dendrimer-RNA dendriplexes.

Notes: Wells were loaded with 10 μ L dendriplex or RNA +2 μ L Thermoscientific Orange DNA Loading Dye. The leftmost lane shows the RNA alone without dendrimer, and the lanes to the right show the dendriplex at the indicated dendrimer:RNA molar ratios. The absence or decrease in fluorescence indicates successful dendriplex formation. Faint fluorescence is visible with dendrimer:RNA ratios of 1:1 and 2:1, while higher ratios (>4:1) show no fluorescence. The concentration of RNA was kept constant in all lanes.

The carboxylated dendrimer facilitated efficient transfection of the oligoribonucleotide decoy into MT4 lymphocytes

The gating for fluorescein uptake was adjusted so that the untreated control showed <1% fluorescence. The dendriplex with \pm charge ratio of 4:1 and 8:1 demonstrated efficient transfection of MT4 lymphocytes on flow cytometry (90.1% and 98.5%, respectively). Dendriplexes with lower charge ratios (2:1 and 1:1) achieved lower transfection

(15.7% and 1.9%, respectively) (Figure 4). By comparison, in other studies, transfection efficiencies of 36% and 90% were reported with the use of a second-generation carbosilane dendrimer in primary T lymphocytes³³ and SupT1 lymphocytes,³⁴ respectively. The RNA alone was taken up by 9.3% of cells.

Removal of surface-bound dendriplexes by an acid-glycine wash suggests that the uptake results represent complexes located within the cell (rather than on the surface of the cell membrane). Omission of the acid-glycine wash resulted in only slight differences in the fluorescence reading (97.6% and 92.6% vs 90.1% and 98.5% for the 4:1 and 8:1 dendriplexes, respectively), suggesting that most of the fluorescence represents intracellular RNA.

Dead cells were identified by staining with Zombie Aqua™ dye. Debris was gated out by its characteristic appearance on side scattered light (SSC)-A and forward scattered light (FSC)-A. The gating was applied so that the Zombie Aqua™ stain correctly determined the viability of untreated cells (~95%) (compared to Trypan Blue staining). Toxicity, based on this gating strategy, was determined to be as follows: RNA only (10 μ M): 9.5%; dendrimer only (54 μ M): 76.5%; dendriplex (8:1): 20.7%; dendriplex (4:1): 10.4%; dendriplex (2:1): 6.4% and dendriplex (1:1): 3.2%.

Uptake was confirmed by confocal microscopy, which furthermore showed the cytoplasmic location of the fluorescent RNA (Figure 5). The dendrimer with charge ratio 2:1 did not show any uptake by confocal microscopy.

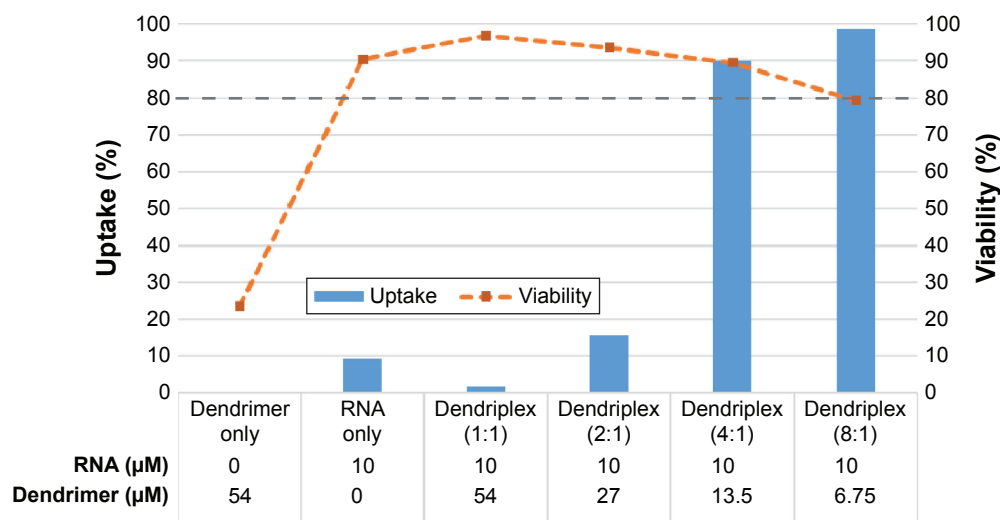


Figure 4 Results of flow cytometry showing RNA uptake and viability of MT4 cells incubated for 4 hours with either RNA or dendrimer alone or with dendriplexes with dendrimer:RNA ratios of 1:1, 2:1, 4:1 and 8:1.

Notes: The RNA was fluorescein labeled. Cells were stained with Zombie Aqua™ dye, fixed and then analyzed by flow cytometry. Surface-bound dendriplexes were removed by an acid-glycine wash. Uptake was quantified as the percentage of cells that were positive for fluorescein, while viability was assessed as the percentage of cells that did not take up the Zombie Aqua™ dye. Uptake of the dendriplex at ratios 1:1, 2:1, 4:1 and 8:1 was 1.9%, 15.7%, 90.1% and 98.5%, respectively. RNA alone had 9.3% uptake. The toxicity of the dendriplex at ratio 8:1 was significantly higher (20.7%) compared to the dendriplex with ratio 4:1 (10.4%) and exceeded the 20% toxicity threshold (shown as - - -). The viability of untreated cells was 95.5%.

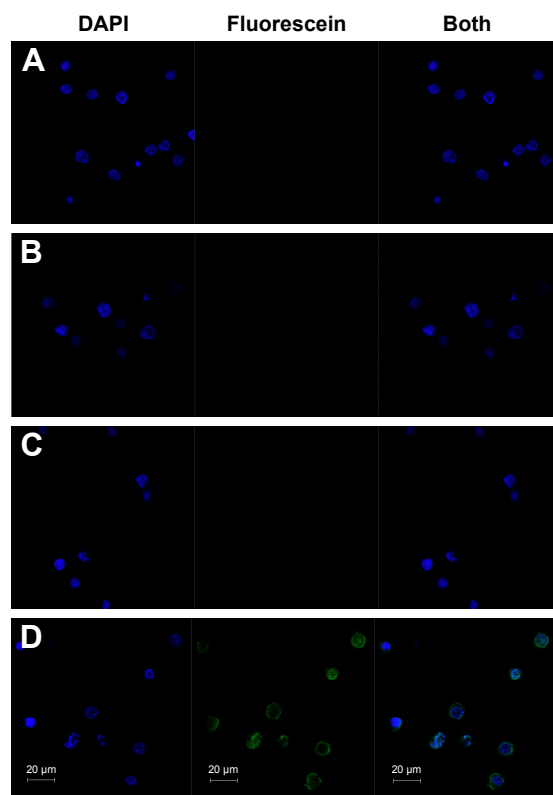


Figure 5 Photograph under confocal microscope of cells incubated overnight with (A) untreated control (RPMI 1640 medium only), (B) RNA control (fluorescent RNA only), (C) Ψ dendriplex at dendrimer:RNA (\pm) charge ratio =2:1, and (D) Ψ dendriplexes at dendrimer:RNA (\pm) charge ratio =4:1.

Abbreviation: RPMI, Roswell Park Memorial Institute.

Cytotoxic and cytoprotective effect of dendriplex and controls

The dendriplex containing the Ψ RNA exhibited a cytoprotective effect and selectivity (IC_{50} =26.8 μ M, EC_{50} =3.20 μ M and SI =8.4), while the RNA alone and the dendriplex containing control RNA had no cytoprotective effect (Figure 6;

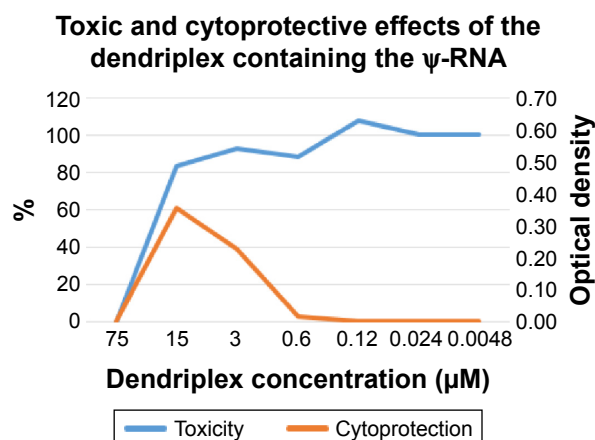


Figure 6 Toxic and cytoprotective effects of the dendriplex (Ψ RNA + dendrimer). **Notes:** The toxic and cytoprotective effects were determined by exposing uninfected and HIV-infected MT4 lymphocytes, respectively, to serial dilutions of the dendriplex containing the Ψ RNA decoy.

Table 1 Toxicity (IC_{50}) and cytoprotective effect (EC_{50}) of Ψ RNA dendriplex and various controls

Treatment	IC_{50} (μ M)	EC_{50} (μ M)	SI (IC_{50}/EC_{50})
AZT (antiviral control)	13.26	0.0023	5,766
Dendriplex	26.8	3.20	8.4
(Ψ RNA + dendrimer)			
RNA alone	Nontoxic*	No effect*	Not calculable*
Dendrimer alone	26.4	No effect*	Not calculable*
Dendriplex	21.7	No effect*	Not calculable*
(control RNA + dendrimer)			

Note: *In the dosage range tested.

Abbreviations: IC_{50} , 50% inhibitory concentration; EC_{50} , 50% effective concentration; SI, selectivity index.

Table 1). The dendriplex with the Ψ RNA restored infected cells to ~60% of the viability of uninfected, untreated cells (Figure 6).

MT4 lymphocytes exposed to the dendriplex retained >80% viability at a dendrimer concentration of 15 μ M (equivalent to 138 μ g/mL). By comparison, peripheral blood mononuclear cells and SupT1 cells exposed to a second-generation carbosilane dendrimer in a study by Weber et al⁵⁶ reached the toxicity limit of 80% at 24 μ g/mL, while in another study, two second-generation dendrimers reached the toxicity limit for macrophages at 5 and 15 μ M, respectively.³³

Viral load assay

HIV-infected lymphocytes treated with the dendriplex did not demonstrate significant reduction in viral load following 3 days of incubation. There was no difference in viral load between the dendriplex containing the Ψ decoy vs control RNA or dendriplex alone without RNA (data not shown). The same result was obtained when the incubation period of the experiment was increased to 5 days.

Discussion

This study showed efficient uptake of a dendrimer-oligoribonucleotide nanocomplex into MT4 lymphocytes with evidence of a cytoprotective effect (EC_{50} =3.20 μ M, SI =8.4) against HIV. However, the dendriplex did not demonstrate significant suppression of HIV viral load. There may be several reasons why the oligoribonucleotide decoy did not have a more profound antiviral and cytoprotective effect. First, interaction of the nucleocapsid protein (NCp7) with the encapsidation signal possibly depends on secondary intermolecular and intramolecular structural motifs rather than a consensus sequence.^{1,2,4} It is not known how well a decoy based on a linear sequence will simulate these motifs. Further studies are required whereby the sequence

and number of nucleotides that constitute the decoy are varied to determine the effect of decoy nucleotide structure on packaging efficiency. Second, there is probably redundancy in NCp7- Ψ interaction,^{24,25,59} ie, more than one stem loop may be able to initiate packaging. To explore this, all four stem loops, singly and in combination, should be evaluated for their anti-packaging effect. Finally, stoichiometry between NCp7 and Ψ may make inhibition challenging. There are $\geq 1,500$ gag molecules per dimerized viral genome.^{5,6,16,59,60} The number of Ψ decoys required to effectively interfere with packaging is not known. Although the dendriplex achieved excellent transfection efficiency, this is not a direct measure of the intracellular Ψ RNA dose (which is limited by the toxicity of the carrier molecule and \pm charge ratios). Furthermore, it is not known whether the RNA is able to exert its activity while bound to the dendrimer, and if not, what proportion is released from the dendriplex once it reaches the cytoplasm.

The cytoprotective effect of the dendriplex was not corroborated by the viral load experiment. This paradoxical outcome could be an artifact of the experimental setup. Further mechanism of action studies will be required to find a suitable explanation. Furthermore, it will be of interest to determine if this finding is replicated with other dendrimers and alternative transfection methods.

We did not study the mechanism of uptake of the dendriplex, which is known to be cell type dependent.⁶¹ Furthermore, we did not assess the rate of uptake, which may be influenced by the cationic nature of the dendrimer.⁶² These are avenues for further research, particularly in lymphocytes that are naturally resistant to transfection.

Conclusion

While this study showed evidence of the cytoprotective effect of a Ψ RNA decoy dendriplex, potent inhibition of encapsidation by this strategy probably requires several issues to be addressed, including optimized design and intracellular delivery of the packaging signal decoy. More importantly, this study provides further evidence that cationic dendrimers may be an efficient non-viral alternative for the delivery of anti-HIV RNA therapeutics into hard-to-transfect lymphocytes.

Acknowledgments

Open access publication of this article has been made possible through support from the Victor Daitz Information Gateway, an initiative of the Victor Daitz Foundation and the University of KwaZulu-Natal. Logan Reddy and staff in the Viral PCR laboratory at the National Health Laboratory Service in Durban for HIV viral loads, Kogi Moodley/Prof

Daniels at the University of KwaZulu-Natal (UKZN) for use of flow cytometry equipment, and Lorika Beukes at UKZN for use of the confocal microscope, are acknowledged. University of Alcalá acknowledges financial support from CTQ2014-54004-P (MINECO) and Consortium NANO-DENDMED ref S2011/BMD-2351 (CM). CIBER-BBN is an initiative funded by the VI National R&D&i Plan 2008–2011, Iniciativa Ingenio 2010, Consolider Program, CIBER Actions and financed by the Instituto de Salud Carlos III with assistance from the European Regional Development Fund. Dr Parboosing received an Academic Fellowship award from the Discovery Foundation of South Africa and funding from the National Research Foundation Thuthuka Program.

Disclosure

The authors report no conflicts of interest in this work.

References

- Lever A. HIV-1 RNA packaging. *Adv Pharmacol*. 2007;55:1–32.
- D'Souza V, Summers MF. How retroviruses select their genomes. *Nat Rev Microbiol*. 2005;3(8):643–655.
- Coffin JM, Hughes SH, Varmus H. *Retroviruses*. Plainview, NY: Cold Spring Harbor Laboratory Press; 1997.
- Fields BN, Knipe DM, Howley PM. *Fields Virology*. 5th ed. Philadelphia, PA: Lippincott Williams & Wilkins; 2007.
- de Rocquigny H, Shvadchak V, Avilov S, et al. Targeting the viral nucleocapsid protein in anti-HIV-1 therapy. *Mini Rev Med Chem*. 2008; 8(1):24–35.
- Goldschmidt V, Miller Jenkins L, de Rocquigny H, Darlix J, Mély Y. The nucleocapsid protein of HIV-1 as a promising therapeutic target for antiviral drugs. *HIV Ther*. 2010;4(2):179–198.
- Roques BP, Morellet N, de Rocquigny H, Demene H, Schueler W, Jullian N. Structure, biological functions and inhibition of the HIV-1 proteins Vpr and NCp7. *Biochimie*. 1997;79(11):673–680.
- Huang M, Maynard A, Turpin JA, et al. Anti-HIV agents that selectively target retroviral nucleocapsid protein zinc fingers without affecting cellular zinc finger proteins. *J Med Chem*. 1998;41(9):1371–1381.
- Rice WG, Supko JG, Malspeis L, et al. Inhibitors of HIV nucleocapsid protein zinc fingers as candidates for the treatment of AIDS. *Science*. 1995;270(5239):1194–1197.
- McBride MS, Panganiban AT. The human immunodeficiency virus type 1 encapsidation site is a multipartite RNA element composed of functional hairpin structures. *J Virol*. 1996;70(5):2963–2973.
- Harrison GP, Miele G, Hunter E, Lever AM. Functional analysis of the core human immunodeficiency virus type 1 packaging signal in a permissive cell line. *J Virol*. 1998;72(7):5886–5896.
- Russell RS, Hu J, Beriault V, et al. Sequences downstream of the 5' splice donor site are required for both packaging and dimerization of human immunodeficiency virus type 1 RNA. *J Virol*. 2003;77(1):84–96.
- Joshi S, Van Brunschot A, Asad S, van der Elst I, Read SE, Bernstein A. Inhibition of human immunodeficiency virus type 1 multiplication by antisense and sense RNA expression. *J Virol*. 1991;65(10):5524–5530.
- Berkhout B, van Wamel JL. Inhibition of human immunodeficiency virus expression by sense transcripts encoding the retroviral leader RNA. *Antivir Res*. 1995;26(2):101–115.
- Joshi S, Ding SF, Liem SE. Co-packaging of non-vector RNAs generates replication-defective retroviral vector particles: a novel approach for blocking retrovirus replication. *Nucleic Acids Res*. 1997;25(16): 3199–3203.

16. Dorman NM, Lever AM. Investigation of RNA transcripts containing HIV-1 packaging signal sequences as HIV-1 antivirals: generation of cell lines resistant to HIV-1. *Gene Ther.* 2001;8(2):157–165.
17. Allen P, Collins B, Brown D, Hostomsky Z, Gold L. A specific RNA structural motif mediates high affinity binding by the HIV-1 nucleocapsid protein (NCp7). *Virology.* 1996;225(2):306–315.
18. Chadwick DR, Lever AM. Antisense RNA sequences targeting the 5' leader packaging signal region of human immunodeficiency virus type-1 inhibits viral replication at post-transcriptional stages of the life cycle. *Gene Ther.* 2000;7(16):1362–1368.
19. Gu S, Ji J, Kim JD, Yee JK, Rossi JJ. Inhibition of infectious human immunodeficiency virus type 1 virions via lentiviral vector encoded short antisense RNAs. *Oligonucleotides.* 2006;16(4):287–295.
20. Harrison G, Lever A. The human immunodeficiency virus type 1 packaging signal and major splice donor region have a conserved stable secondary structure. *J Virol.* 1992;66(7):4144.
21. Shubsda MF, Paoletti AC, Hudson BS, Borer PN. Affinities of packaging domain loops in HIV-1 RNA for the nucleocapsid protein. *Biochemistry.* 2002;41(16):5276–5282.
22. Paoletti AC, Shubsda MF, Hudson BS, Borer PN. Affinities of the nucleocapsid protein for variants of SL3 RNA in HIV-1. *Biochemistry.* 2002;41(51):15423–15428.
23. Clever JL, Taplitz RA, Lochrie MA, Polisky B, Parslow TG. A heterologous, high-affinity RNA ligand for human immunodeficiency virus Gag protein has RNA packaging activity. *J Virol.* 2000;74(1):541–546.
24. De Guzman RN, Wu ZR, Stalling CC, Pappalardo L, Borer PN, Summers MF. Structure of the HIV-1 nucleocapsid protein bound to the SL3 psi-RNA recognition element. *Science.* 1998;279(5349):384–388.
25. Zeffman A, Hassard S, Varani G, Lever A. The major HIV-1 packaging signal is an extended bulged stem loop whose structure is altered on interaction with the Gag polypeptide. *J Mol Biol.* 2000;297(4):877–893.
26. Dorman N, Lever AM. RNA-based gene therapy for HIV infection. *HIV Med.* 2001;2(2):114–122.
27. Huang A. Defective interfering viruses. *Annu Rev Microbiol.* 1973;27(1):101–118.
28. Darlix JL, Garrido JL, Morellet N, Mely Y, de Rocquigny H. Properties, functions, and drug targeting of the multifunctional nucleocapsid protein of the human immunodeficiency virus. *Adv Pharmacol.* 2007;55:299–346.
29. Dawson L, Yu XF. The role of nucleocapsid of HIV-1 in virus assembly. *Virology.* 1998;251(1):141–157.
30. Bampi C, Jacquenet S, Lener D, Decimo D, Darlix JL. The chaperoning and assistance roles of the HIV-1 nucleocapsid protein in proviral DNA synthesis and maintenance. *Int J Biochem Cell Biol.* 2004;36(9):1668–1686.
31. Reslan L, Mestas J-L, Herveau S, Béra J-C, Dumontet C. Transfection of cells in suspension by ultrasound cavitation. *J Control Release.* 2010;142(2):251–258.
32. Ramishetti S, Kedmi R, Goldsmith M, et al. Systemic gene silencing in primary T lymphocytes using targeted lipid nanoparticles. *ACS Nano.* 2015;9(7):6706–6716.
33. Perise-Barrios AJ, Jimenez JL, Dominguez-Soto A, et al. Carbosilane dendrimers as gene delivery agents for the treatment of HIV infection. *J Control Release.* 2014;184:51–57.
34. Gonzalo T, Clemente M, Chonco L, et al. Gene therapy in HIV-infected cells to decrease viral impact by using an alternative delivery method. *ChemMedChem.* 2010;5(6):921–929.
35. Popovic M, Sarngadharan MG, Read E, Gallo RC. Detection, isolation, and continuous production of cytopathic retroviruses (HTLV-III) from patients with AIDS and pre-AIDS. *Science.* 1984;224(4648):497–500.
36. Ratner L, Haseltine W, Patarca R, et al. Complete nucleotide sequence of the AIDS virus, HTLV-III. *Nature.* 1985;313(6000):277–284.
37. Aldovini A, Young RA. Mutations of RNA and protein sequences involved in human immunodeficiency virus type 1 packaging result in production of noninfectious virus. *J Virol.* 1990;64(5):1920–1926.
38. Berkowitz RD, Goff SP. Analysis of binding elements in the human immunodeficiency virus type 1 genomic RNA and nucleocapsid protein. *Virology.* 1994;202(1):233–246.
39. Clavel F, Orenstein JM. A mutant of human immunodeficiency virus with reduced RNA packaging and abnormal particle morphology. *J Virol.* 1990;64(10):5230–5234.
40. Clever JL, Parslow TG. Mutant human immunodeficiency virus type 1 genomes with defects in RNA dimerization or encapsidation. *J Virol.* 1997;71(5):3407–3414.
41. Kaye JF, Richardson JH, Lever AM. cis-acting sequences involved in human immunodeficiency virus type 1 RNA packaging. *J Virol.* 1995;69(10):6588–6592.
42. Kim HJ, Lee K, O'Rear JJ. A short sequence upstream of the 5' major splice site is important for encapsidation of HIV-1 genomic RNA. *Virology.* 1994;198(1):336–340.
43. Lever A, Gottlinger H, Haseltine W, Sodroski J. Identification of a sequence required for efficient packaging of human immunodeficiency virus type 1 RNA into virions. *J Virol.* 1989;63(9):4085–4087.
44. Sakaguchi K, Zambrano N, Baldwin ET, et al. Identification of a binding site for the human immunodeficiency virus type 1 nucleocapsid protein. *Proc Natl Acad Sci U S A.* 1993;90(11):5219–5223.
45. Berglund JA, Charpentier B, Rosbash M. A high affinity binding site for the HIV-1 nucleocapsid protein. *Nucleic Acids Res.* 1997;25(5):1042–1049.
46. Turner KB, Hagan NA, Fabris D. Inhibitory effects of archetypical nucleic acid ligands on the interactions of HIV-1 nucleocapsid protein with elements of Psi-RNA. *Nucleic Acids Res.* 2006;34(5):1305–1316.
47. Clever J, Sassetti C, Parslow TG. RNA secondary structure and binding sites for gag gene products in the 5' packaging signal of human immunodeficiency virus type 1. *J Virol.* 1995;69(4):2101–2109.
48. Dannull J, Surovoy A, Jung G, Moelling K. Specific binding of HIV-1 nucleocapsid protein to PSI RNA in vitro requires N-terminal zinc finger and flanking basic amino acid residues. *EMBO J.* 1994;13(7):1525–1533.
49. Hagan N, Fabris D. Direct mass spectrometric determination of the stoichiometry and binding affinity of the complexes between nucleocapsid protein and RNA stem-loop hairpins of the HIV-1 Psi-recognition element. *Biochemistry.* 2003;42(36):10736–10745.
50. Vuilleumier C, Bombarda E, Morellet N, Gerard D, Roques BP, Mely Y. Nucleic acid sequence discrimination by the HIV-1 nucleocapsid protein NCp7: a fluorescence study. *Biochemistry.* 1999;38(51):16816–16825.
51. ThermoScientific. *Thermo Scientific Deprotection 2'-ACE Protected RNA.* Available from: http://dharmacon.gelifesciences.com/uploadedFiles/Products/Custom_Synthesis/Single-stranded_RNA_Synthesis/deprotection-protocol.pdf. Accessed May 8, 2014.
52. Fuentes-Paniagua E, Hernandez-Ros JM, Sanchez-Milla M, et al. Carbosilane cationic dendrimers synthesized by thiol-ene click chemistry and their use as antibacterial agents. *RSC Adv.* 2014;4(3):1256–1265.
53. Pannecouque C, Daelemans D, De Clercq E. Tetrazolium-based colorimetric assay for the detection of HIV replication inhibitors: revisited 20 years later. *Nat Protoc.* 2008;3(3):427–434.
54. World Health Organization [webpage on the Internet]. *Laboratory Biosafety Manual.* 3rd ed. 2004. Available from: http://www.who.int/csr/resources/publications/biosafety/WHO_CDS_CSR_LYO_2004_11/en/. Accessed November 10, 2016.
55. Centers for Disease Control [webpage on the Internet]. *Biosafety in Microbiological and Biomedical Laboratories (BMBL).* 5th ed. 2009. Available from: <http://www.cdc.gov/biosafety/publications/bmb15/>. Accessed November 10, 2016.
56. Weber N, Ortega P, Clemente MI, et al. Characterization of carbosilane dendrimers as effective carriers of siRNA to HIV-infected lymphocytes. *J Control Release.* 2008;132(1):55–64.
57. Kameyama S, Horie M, Kikuchi T, et al. Acid wash in determining cellular uptake of Fab/cell-permeating peptide conjugates. *Biopolymers.* 2007;88(2):98–107.
58. Jimenez JL, Clemente MI, Weber ND, et al. Carbosilane dendrimers to transfect human astrocytes with small interfering RNA targeting human immunodeficiency virus. *BioDrugs.* 2010;24(5):331–343.

59. Amarasinghe GK, De Guzman RN, Turner RB, Chancellor KJ, Wu ZR, Summers MF. NMR structure of the HIV-1 nucleocapsid protein bound to stem-loop SL2 of the psi-RNA packaging signal. Implications for genome recognition. *J Mol Biol.* 2000;301(2):491–511.
60. Musah RA. The HIV-1 nucleocapsid zinc finger protein as a target of antiretroviral therapy. *Curr Top Med Chem.* 2004;4(15):1605–1622.
61. Manunta M, Nichols BJ, Tan PH, Sagoo P, Harper J, George AJ. Gene delivery by dendrimers operates via different pathways in different cells, but is enhanced by the presence of caveolin. *J Immunol Methods.* 2006;314(1–2):134–146.
62. Marquez-Miranda V, Penaloza JP, Araya-Duran I, et al. Effect of terminal groups of dendrimers in the complexation with antisense oligonucleotides and cell uptake. *Nanoscale Res Lett.* 2016;11(1):66.

International Journal of Nanomedicine

Publish your work in this journal

The International Journal of Nanomedicine is an international, peer-reviewed journal focusing on the application of nanotechnology in diagnostics, therapeutics, and drug delivery systems throughout the biomedical field. This journal is indexed on PubMed Central, MedLine, CAS, SciSearch®, Current Contents®/Clinical Medicine,

Submit your manuscript here: <http://www.dovepress.com/international-journal-of-nanomedicine-journal>

Journal Citation Reports/Science Edition, EMBase, Scopus and the Elsevier Bibliographic databases. The manuscript management system is completely online and includes a very quick and fair peer-review system, which is all easy to use. Visit <http://www.dovepress.com/testimonials.php> to read real quotes from published authors.

Dovepress